26th EPS Conf. on Contr. Fusion and Plasma Physics, Maastricht, 14 - 18 June 1999 ECA Vol.23J (1999) 217 - 220

Argon in JET Optimised Shear Plasmas

K-D Zastrow, H Anderson[1], C Jupén[2], M G von Hellermann, A C Maas, M G O'Mullane[1], B Alper, Yu F Baranov, A J Bickley, D Borba[3], C D Challis, G D Conway, N Deliyanakis, C Gormezano, C W Gowers, N C Hawkes[4], T C Hender[4], L C Ingesson, E Joffrin[5], T T C Jones, P J Lomas, M J Mantsinen[6], F G Rimini, A C C Sips, F X Söldner, M F Stamp

JET Joint Undertaking, Abingdon, United Kingdom
[1]Department of Physics and Applied Physics, University of Strathclyde, UK
[2]Department of Physics, Lund University, Sweden
[3]Associação EURATOM/IST, Inst Superior Tecnico, Lisbon, Portugal
[4]Euratom/UKAEA Fusion Association, Culham Science Centre, Abingdon, UK
[5]Association EURATOM-CEA, CEA-Cadarache, France
[6]Helsinki University of Technology, Association EURATOM-TEKES, Finland

ABSTRACT AND INTRODUCTION

During the JET Mark IIGB campaign Argon radiation has been used to control the edge (resulting in type III ELMs or L-Mode edge) and to prolong the duration of optimised shear (OS) discharges with internal transport barriers (ITBs) [1,2]. This results in weak barriers less prone to disruptions. The best discharges maintain quasi steady-state conditions for up to 3 energy confinement times with neutron yields up to equivalent Q_{DT}≈0.4 at typical β_N≈2.

In these discharges Argon accumulates in the core region with typical dilution of n_d/n_e≅0.7 and Z_{eff} on axis up to 4.5, with contributions from Argon of $\Delta n_d/n_e$≅-0.2 and ΔZ_{eff}≅3. There are indications that the Argon concentration would saturate at a higher level, if the discharges were further extended. Transport analysis shows that the accumulation is due to a strong inward convection in the ITB region, combined with a weak inward convection in the core.

CXS DATA ANALYSIS AND DATA CONSISTENCY

The amount of Argon necessary to achieve radiated power fractions of the order 20-40% affects the charge exchange spectroscopy (CXS) spectra in the vicinity of the C^{+5}(n=8-7) transition that is used to infer ion temperature, toroidal rotation and carbon concentration. There are 21 individual spectral lines of Ar^{+1} (some of these emanate from identified multiplets) in the wavelength range from 522 nm to 532 nm, and one transition from Ar^{+5}. At JET we have three instruments available for recording this spectrum, two horizontal arrays and one vertical line-of-sight. The two horizontal arrays view the plasma in the co and counter rotation direction, respectively. Due to the Doppler shift, active charge exchange features are therefore located in different spectral regions which results in different systematic errors in the interpretation for each instrument.

Without the presence of Argon, there is generally good agreement between all three instruments on the absolute values of temperature, rotation and carbon density. With Argon, significant discrepancies emerge (Fig. 1). One of the horizontal profile instruments has an extended wavelength range that covers the Ar^{+17}(n=16-15) transition. This too is blended with spectral lines from Ar^{+1}, and therefore the accuracy of ion temperature and rotation measurements is not enhanced due to its inclusion in the analysis. Also shown in Fig. 1 is the density of fully stripped Argon from this instrument. Note that in strong barrier discharges, the

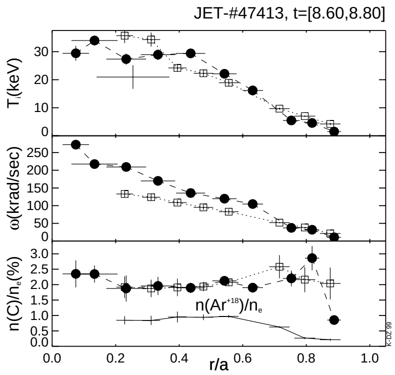

Fig. 1: Simultaneous results from all CXS instruments in OS discharges with Argon. The spectral analysis is ambiguous due to Ar^{+1} emission from the plasma edge. Without Argon results agree within error bars.

Carbon concentration profile is hollow since the Carbon density profile is flat. In weak barrier discharges the density profile is peaked, which results in the observed flat concentration profile. For the data in Fig. 1, the dilution has reached $n_d/n_e \cong 0.7$ and Z_{eff} on axis is close to 4.5, with contributions from Argon of $\Delta n_d/n_e \cong -0.2$ and $\Delta Z_{eff} \cong 3$.

In optimised shear discharges without Argon, the data consistency is generally acceptable. The volume integrals of electron and ion pressure plus the contributions from NBI and RF heating as modelled by the PION code [3] add up to the measured W_{Dia}. The neutron yield is generally overpredicted, but the amount remains within the expected errors. With Argon, the model for W_{Dia} still is satisfactory, however there is no room for any neutron emission from RF, once thermal-thermal yield and slowing down beam-thermal yield are considered. There should be an additional yield (up to 30%) from RF acceleration of the beam ion tail [4]. This suggests that T_i is in fact lower than measured, or the dilution is underestimated.

ATOMIC MODELLING

The spectral emission from Ar^{+17}(n=16-15) following electron capture from beam neutrals is utilised to infer the concentration of Ar^{+18}. For this use effective beam stopping and charge exchange emission coefficients are required. Beam stopping coefficients are used to

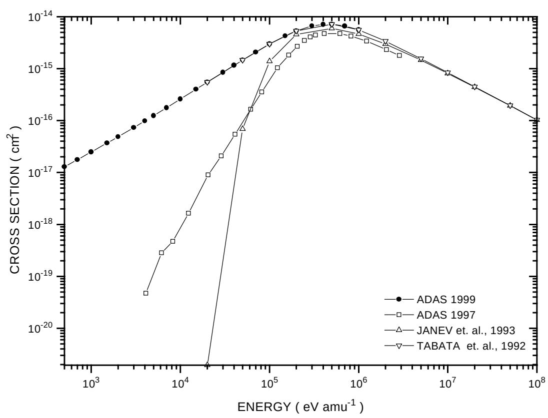

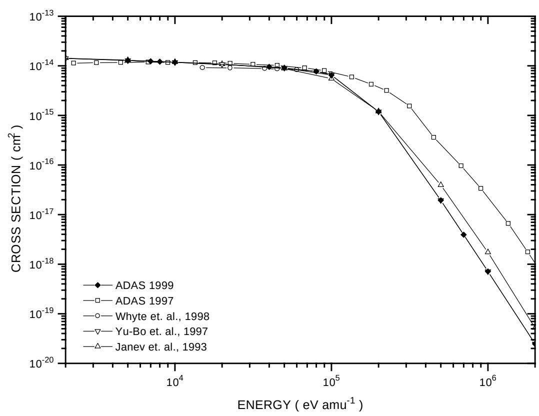

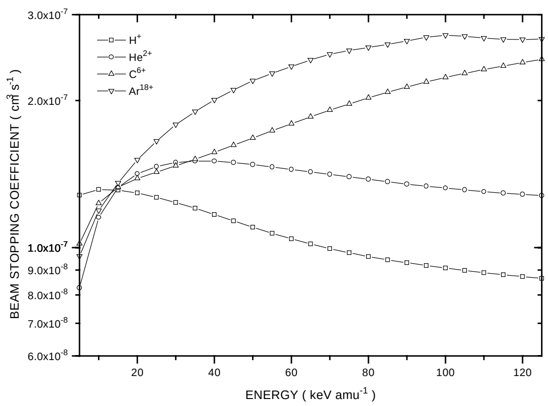

Fig. 2: Top left: Impact ionisation cross sections as a function of energy for neutral hydrogen colliding with Ar^{18+}. Top right: Total charge exchange cross sections. The curves labeled ADAS 1999 are the cross sections used in this paper. Left: Behaviour of the beam stopping coefficient for a range of pure impurity plasmas. The electron density is 3.0 x 10^{19} m^{-3} with the condition of charge neutrality imposed. The ion temperature is 2 keV. The increase of the beam stopping coefficient with nuclear charge can clearly be observed.

calculate the beam attenuation, while the charge exchange emission coefficients are required to extract the concentration of Ar^{18+} from the recorded charge exchange flux. The effective beam stopping coefficients in a composite plasma are evaluated with a bundled-nS collisional-radiative model from the Atomic Data and Analysis Structure package, (ADAS [5]). Ar^{18+} as a plasma impurity species had not been considered before and it was necessary to assess the fundamental cross section data for ion impact ionisation, excitation, total charge transfer and effective charge exchange emission coefficients for the Ar^{17+}(n=16-15) transition [6,7,8,9].

One interesting outcome of this model is the increase of the beam stopping coefficient with nuclear charge (Fig. 2) which means that the core heating efficiency from the beams will be reduced in the presence of Argon.

ARGON ACCUMULATION AND TRANSPORT ANALYSIS

In strong barrier discharges, the Carbon concentration drops after the barrier is formed, while the Carbon density remains roughly constant. In weak barrier discharges with Argon, on the other hand, the Carbon concentration remains constant, while the Carbon density increases. A continuous increase of the Argon concentration and density is also observed. These results are consistent with previous observations on C and Ni [10].

The Argon influx is described by a two reservoir model, consisting of the plasma and a second volume that incorporates the pipework, subdivertor volume and pump. The Argon source from the valves is taken from the calibration of the gas supply. The influx is monitored by making use of the time history of Ar^{+5} line emission in our CXS spectra (Fig. 3). The pump rate (4/s) of the two-reservoir model is chosen to match the intensity decay of this spectral line after the Argon dosing is turned off. Additionally a fuelling rate is needed to connect this external reservoir to the observed plasma volume as well as edge transport parameters. The combined effect of these coefficients is chosen to match the time evolution of the outermost measured density. The source rate of ions into the observed volume (r/a<0.9) is thus

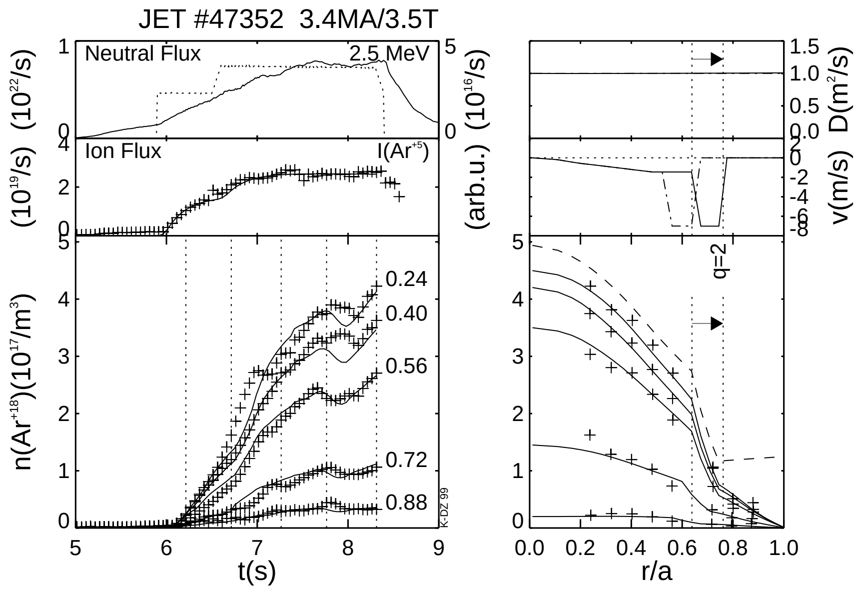

Fig. 3: Result of Argon transport analysis for JET discharge 47352. Top left: neutron yield and Argon dosing waveform. Left: Ion flux from two reservoir model (---) and observed intensity of low Argon ionisation stage (+), representative of the Argon influx. Bottom left: Ar^{+18} density at 5 normalised minor radii vs time (+ Data ---- Transport model). Top right: Diffusion coefficient, assumed constant in radius for simplicity. Right: Convection velocity. Bottom right: Ar^{+18} density at 5 times vs normalised minor radius. Also marked is the radial location of the q=2 surface at the first and last time. (+ Data ---- Transport model - - - Total Argon density at the last time slice, summing over all ionisation stages).

equivalent to 0.25/s, or an effective fuelling efficiency of 0.3%. Typically the discharges reach $\tau_{Ar}(r/a<0.9)\approx 1\text{-}2\ \tau_E$ after about one energy confinement time.

In this paper results of Argon transport analysis are presented for #47352, since $\tau_{Ar}\approx\tau_E$ for all times. This allows the use of a transport model with transport parameters that are constant in time. For most discharges the transport cannot be simplified to this level, since either the fuelling varies due to changes in plasma configuration or the transport changes.

The diffusion coefficient is set constant in radius, D=1 m^2/s for simplicity. If D is chosen much lower (0.5 m^2/s) there is not enough Argon available for the first 900 ms after the Argon puff is applied to fill the core at the observed rate. If D is chosen much larger (2 m^2/sec), additional loss terms are required (for example outward convection) which are inconsistent with the observed profile shape.

The convection term is used exclusively to model the density profile evolution. While small variations of D with radius can be compensated for by changes in convection to give the same overall result, some features are resilient. Since there are no internal sources of Argon, the peaked density profile in the core requires a finite inward convection term. Equally, the strong Ar^{+18} density gradient in the ITB region requires a strong inward convection term. This region is modelled by locating a 15 cm wide interval with large convection velocity just inside the radius of the q=2 surface as given by EFIT. In the model, the q=2 surface is followed in time. This gives the most consistent density profile with respect to the density measurements. If the barrier width was different, the magnitude of the inward convection would have to be changed accordingly. The model is only sensitive to the product of width and convection velocity.

One outcome of this model is the calculation of the density of additional Argon ionsation stages. In the core, lower ionisation stages (mainly Ar^{+17}) amount to about 10% of the measured Ar^{+18}. Outside the ITB region, the sum over all lower ionisation stages is about the same as the observed Ar^{+18} density. These results are not yet incorporated in the data consistency calculations.

SUMMARY

Argon radiation has been used to control the edge and to prolong the duration of discharges with ITBs by promoting weak barriers less prone to disruptions. The amounts that are required to do this have a detrimental effect on the data quality from the CXS diagnostic, and hence overall data consistency. In contrast to strong barrier discharges, impurities (Carbon and Argon) accumulate in the core region with typical dilution of $n_d/n_e\cong 0.7$ and Z_{eff} on axis up to 4.5, with contributions from Argon of $\Delta n_d/n_e\cong -0.2$ and $\Delta Z_{eff}\cong 3$. Transport analysis shows that the accumulation is due to a strong inward convection in the ITB region of the discharge, combined with a weak inward convection in the core.

The experience from these experiments is that a radiative mantle combined with an optimised shear plasma core leads to degradation of the plasma purity, most likely due to a transport mechanism that is intimately linked with the improved confinement.

[1] Sips, A C C et al., this conference [2] Söldner, F X et al., this conference
[3] Eriksson, L-G, et al., Nuclear Fusion Vol. 33, 1993, p. 1037
[4] Mantsinen, M J, et al., to appear in Plasma Physics and Controlled Fusion
[5] Summers, H. P., JET Joint Undertaking internal report, JET-IR(94)06, 1994.
[6] Tabata, T., et al., Plasma-Mater. Inter. Data Fusion, Vol. 2, 1992, p. 91
[7] Janev, R. K., and Smith, J.J., Plasma-Mater. Inter. Data Fusion, Vol. 4, 1993, p. 1
[8] Yu-Bo, Q., et al., J. Phys. B, Vol. 30, 1997, p. 1955
[9] Whyte, D. G., et al., Physics of plasmas, Vol.5, No. 10, 1998, p. 3694
[10] Chen, H, et al, EPS Conference on Contr. Fusion, 1998, Prague